

Next-step spherical torus experiment and spherical torus strategy in the course of development of fusion energy

M. Ono¹, M. Peng², C. Kessel¹, C. Neumeyer¹, J. Schmidt¹,
J. Chrzanowski¹, D. Darrow¹, L. Grisham¹, P. Heitzenroeder¹,
T. Jarboe³, C. Jun¹, S. Kaye¹, J. Menard¹, R. Raman³,
T. Stevenson¹, M. Viola¹, J. Wilson¹, R. Woolley¹ and I. Zatz¹

¹ Princeton Plasma Physics Laboratory, Princeton, NJ, USA

² Oak Ridge National Laboratory, Oak Ridge, TN, USA

³ University of Washington, Seattle, WA, USA

E-mail: mono@pppl.gov

Received 7 November 2002, accepted for publication 9 January 2004

Published 1 March 2004

Online at stacks.iop.org/NF/44/452 (DOI: 10.1088/0029-5515/44/3/011)

Abstract

A spherical torus (ST) fusion energy development path which is complementary to the proposed tokamak burning plasma experiments such as ITER is described. The ST strategy focuses on a compact component test facility (CTF) and high performance advanced regimes leading to more attractive Demo and power plant scale reactors. To provide the physical basis for the CTF an intermediate step needs to be taken, which we refer to as the ‘next-step spherical torus’ (NSST) device and which we examine in some detail herein. NSST is a ‘performance extension’ stage ST with a plasma current of 5–10 MA, $R = 1.5$ m, $B_T \leq 2.6$ T and the possibility of varying physical parameters. The mission of NSST is to (1) provide a sufficient physical basis for the design of a CTF; (2) explore advanced operating scenarios with high bootstrap current fraction and high performance which can be utilized by CTF, Demo, and power plants; and (3) contribute to the general science of high β toroidal plasmas. The NSST is designed to utilize a TFTR-like site to minimize the cost and time required for design and construction.

PACS numbers: 52.55.Fd, 28.52.Av, 52.25.Xz

1. Spherical torus contributions towards developing fusion energy

The potential of the spherical torus (ST) configuration to contribute to the development of fusion energy was discussed in a number of recent papers [1–3]. The engineering feasibility of a single-turn centre leg for the toroidal field (TF) coils was identified as a key element for useful ST reactors [1]. It should be noted that for ST plasmas the plasma current and the TF coil current are comparable, thus making the single-turn TF concept practical. The single turn design avoids the use of insulators in the centre column, which in turn greatly reduces the shielding requirements. This type of simple TF centre column leads to a very compact component test facility (CTF) (sometimes referred to as the volume neutron source (VNS)) with $R \sim 1$ –1.5 m [2, 3] assuming standard ST physics performance (such as $\beta_T \sim 15$ –25%) to produce substantial neutron wall loading ($W_L \sim 1$ MW m⁻² or higher) at a modest total fusion power (~ 50 MW or higher). The mission of the CTF would be to conduct tests and develop

reliable, high performance fusion nuclear components [4] for an attractive Demo power plant. The key requirements for the realization of a compact CTF with minimal inboard shielding, are that the centre column cannot contain an Ohmic solenoid and cannot utilize insulating materials, as would be required for any multi-turn TF or OH coil. The solenoid-less plasma start-up demonstrated at the multi-MA level is, therefore, an important aim of the next-step spherical torus (NSST) experiment, as described in this manuscript. Finally, we note that the minimization of the total fusion power (thus the tritium usage) is an important consideration for a CTF facility because the availability of tritium fuel will become limited in the coming decades.

The critical nature of the CTF in the accelerated development of fusion energy was recently recognized more broadly in the US fusion research community. For example, the preliminary report of the fusion development path panel under the US Fusion Energy Science Advisory Committee [5] states that ‘within the MFE (magnetic fusion energy) path, a significant experience is anticipated from testing

plasma support technologies (e.g. superconducting magnets and plasma heating) in ITER. However testing of chamber technology in ITER is limited by the relatively low plasma duty cycle and the lower flux neutron fluence than encountered in Demo. Thus, a CTF is judged to be necessary in addition to a burning plasma experiment in order for Demo to meet its goals for tritium self-sufficiency, and practical, safe, and reliable engineering operation with high thermodynamic efficiency, rapid remote maintenance and high availability.’ The report further notes that ‘since the Demo is to demonstrate the operation of an attractive fusion system, it must not itself devoted to testing components for the first time in a fully realistic fusion environment. Furthermore, the tritium consumption of a large facility such as Demo makes it impractical for developing tritium breeding components, as only very little operation without full breeding would be possible.’ One can, therefore, envision that a CTF facility would begin the operation at a modest level of neutron wall loading of $W_L \sim 1\text{--}2\text{ MW m}^{-2}$, and progressively upgrade the test components to handle higher W_L while improving ST plasma performance with the physics input from NSST. As a nuclear facility, the CTF device is expected to satisfy stringent operational requirements [3], such as complete modularity of all fusion core components (including the single-turn centre leg) to permit rapid change for replacement under fully remote conditions. The CTF device should also achieve the high neutron fluence ($\sim 6\text{ MW yr m}^{-2}$ or higher) required in the testing programme.

The significant amount of tritium required for component testing puts a premium on compact devices that maximize W_L while minimizing the total fusion power. Due to a shortage in the supply of tritium anticipated over the next few decades, net tritium consumption by CTF must be carefully managed. Towards this end, the fusion neutrons lost to the centre leg should be minimized while maximizing the tritium capture and breeding ratios of the outboard blanket components. This consideration tends to drive the CTF design towards lower aspect ratios [1]. Such a compact CTF with high fusion and external drive powers is expected to lead to very high plasma heat and particle fluxes on the plasma facing components (PFCs). The development of reliable high performance fusion blanket modules and PFCs under fusion nuclear conditions to aid an attractive Demo design will, therefore, be an overarching goal of the CTF programme.

Effective and accelerated development of fusion energy using key contributions from the ST can, therefore, be envisioned as shown in figure 1. The schematics of three representative ST devices, NSTX, NSST, and a version of CTF, are shown in figure 2; some key parameters for these three devices are listed in table 1. As illustrated in figure 1, the ST development path starts with the on-going proof-of-principle (PoP) level ST experiments (e.g. NSTX, MAST) to establish the physical principles of the ST concept at the $I_p \approx 1\text{ MA}$ level. A performance extension (PE) level ST experiment (NSST) with $I_p = 5\text{--}10\text{ MA}$ is needed to provide the ST physics database for fusion plasma parameters, including the physics of alpha-particles at high beta with a significant fusion gain of $Q \geq 2$. Early in its operations, NSST will develop the physical basis required to design and construct a compact CTF device without an Ohmic solenoid. This includes a

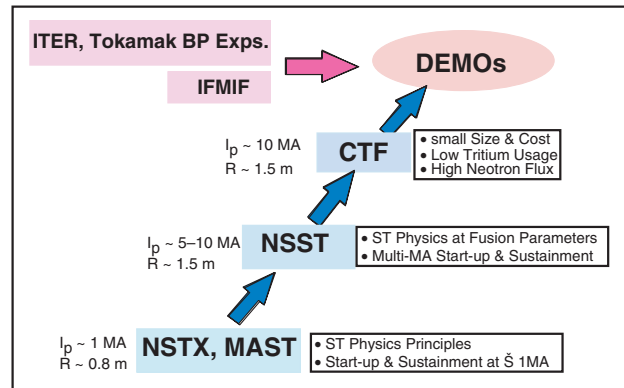


Figure 1. ST contribution to the development of fusion energy. The present experimental devices including NSTX/MAST provide a physics database for the design of NSST. The NSST operating at 5–10 MA at fusion parameters provides the necessary physical basis for CTF and high beta physics data for Demo. The CTF facility is dedicated to develop high performance reliable core components for Demo.

demonstration of multi-MA solenoid-free start-up and non-inductive sustainment. Once the CTF physics feasibility demonstration is achieved on NSST, the CTF engineering design and construction can proceed at a separate nuclear site. The NSST facility can then continue to explore more advanced ST regimes to raise the plasma performance in CTF and help optimize the design of Demo. The initial CTF fusion blanket and other core components can utilize the ITER core technology and component designs, and benefit from the materials developed by IFMIF. The ST development path via CTF would, therefore, complement the tokamak burning plasma experiments, such as ITER, and the material testing facility, such as IFMIF, in order to optimize the Demo design.

As indicated in table 1, the plasma and device parameters increase significantly, by nearly an order of magnitude, from the existing 1 MA class devices represented by NSTX and MAST to the 10 MA class NSST. However, being a physics-oriented facility, the design philosophy of NSST is quite similar to that of NSTX and MAST, namely to maximize the device’s physics capabilities (physics tools as well as ample diagnostic access) with an effective use of existing site credits to minimize construction cost and time. On the other hand, while the plasma parameters are similar to NSST, the CTF facility is designed with the mission of testing and developing advanced core components for Demo and power plants in a nuclear environment. While NSST is an inherently pulsed device, the CTF operates at steady-state. The schematics in figure 2 illustrate the engineering and technology design contrasts for NSST and CTF. Because of the nuclear and engineering constraints, the CTF facility will be quite limited in terms of the physical tools and diagnostic capabilities, compared to NSST.

2. Mission and basic device design parameters of NSST

2.1. Next-step PE ST

NSST is envisioned as a PE stage ST with $I_p \times A \approx 8\text{--}16\text{ MA}$, which is similar to PE tokamaks such as JET, JT-60, and

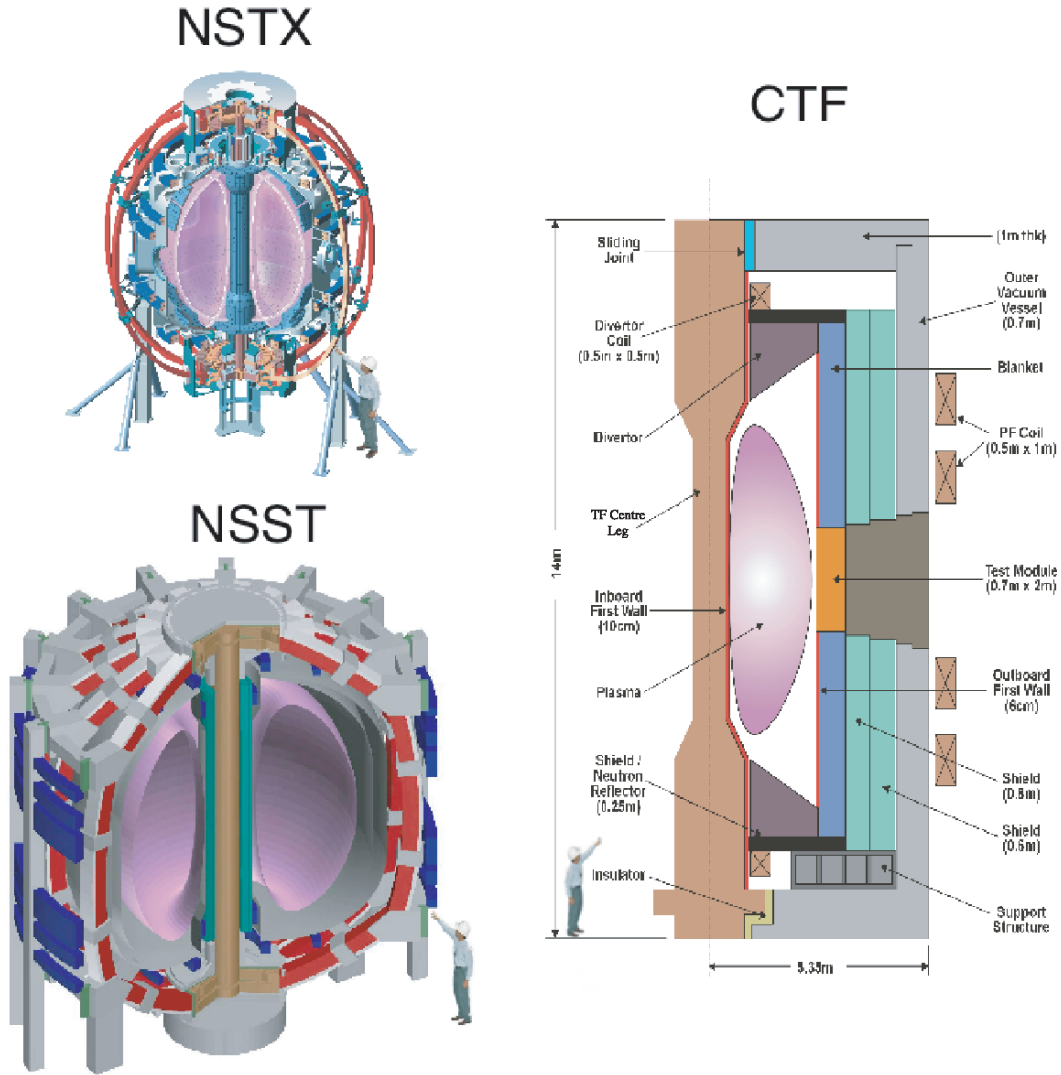


Figure 2. Representative ST device schematics. The NSTX device at 1.5 MA is a PoP step to demonstrate the attractiveness of the ST concept. The NSST at 5–10 MA is a performance-extension step to demonstrate the physical viability of ST at fusion parameters. The CTF is envisioned to be a single-turn-TF steady-state ST device with compact size and modest tritium consumption (~100 MW).

Table 1. Key device and plasma parameters for three representative devices for the ST fusion energy development path.

	NSTX	NSST	CTF
R (m)	0.85	1.5	1–1.5
a (m)	0.65	~0.9	~0.7–1
κ, δ	2, 0.8	~2.7, ~0.6	~3, ~0.5
I_p (MA)	1.5	~5–10	~10–12
B_T (T)	0.3–0.6	~1.1–2.6	~1.7–2.1
Pulse (s)	5–1	~50–5	Steady-state
TF	Multi-turn	Multi-turn	Single-turn

TFTR. It should be noted that the quantity $I_p \times A$ has been used as an approximate indicator of the tokamak device performance, $n \times \tau \times T$ [6]. The I_p dependence signifies the importance of the plasma current in device performance, and the aspect-ratio ‘ A ’ reflects the unfavourable effect of toroidicity on confinement. Interestingly, the original 1984 paper [5] based on the so-called L-mode scaling predicted

stronger toroidicity scaling of $\sim I_p \times A^{1.2}$ whereas more modern ITER confinement scaling (e.g. ITER-89P) tends to predict a somewhat weaker toroidicity dependence of $\sim I_p \times A^{0.8}$. Obviously, having an extensive confinement data base for low values of A from ST experiments would be an advantage for an understanding of the overall toroidal fusion physics.

2.2. NSST mission

The primary mission elements of NSST are to conduct ST research at fusion plasma parameters to

- (1) provide a sufficient physical basis for the design of a compact CTF,
- (2) explore advanced physics and operating scenarios with high bootstrap current fraction/high performance, sustained, advanced ST regimes, which can then be utilized on CTF, Demo, and/or power plants, and

- (3) contribute to the general plasma/fusion science of high β toroidal plasmas including astrophysics.

2.3. Recent progress on the ST database

For NSST and future ST facilities, it is crucial to have an adequate experimental database as well as the relevant theory and modelling to be able to predict the plasma performance. Indeed, the progress in ST plasma research worldwide has been quite rapid and encouraging [7, 8]. In the area of high beta operations, the high average toroidal beta values of $\langle\beta_T\rangle \sim 35\%$ were achieved at a high plasma current of $I_p \sim 1.2$ MA with a stored energy of $E_T \sim 200$ kJ on NSTX [9], which is a significant advance over the previous START high beta results obtained with $I_p \sim 0.2$ MA with $E_T \sim 20$ kJ [10]. Also in NSTX, high normalized beta values of $\beta_N \leq 6.5$ ($\beta_N \leq 10 I_i$) were achieved where the so-called no-wall beta limits were significantly exceeded by about 35% [11]. In the area of plasma confinement, the observed global plasma energy confinement time in the neutral beam injection (NBI) heated NSTX and MAST plasmas exceeded the conventional confinement scalings both for H-mode and L-mode, diverted as well as inboard-limited plasmas [8, 12]. In figure 3, the global H-mode confinement data obtained in NSTX during the quasi-stationary phase of a discharge is shown. The red points are the experimental confinement time computed from the global stored energy, from EFIT reconstruction and the input heating power. The green points show a more recent assessment of the thermal plasma confinement time, where the energy component and the prompt beam loss components have been estimated by the TRANSP modelling code [12]. The NSST base performance projection assumes $HH = 1.3$ – 1.4 to obtain $Q = 2$ performance. The NSST Q performance is strongly dependent on the HH value, so it is clear that the confinement and transport areas are important research areas for STs. In the area of integration, high poloidal-beta H-mode discharges ($\varepsilon\beta_p \sim 1$) at 800 kA were obtained with a

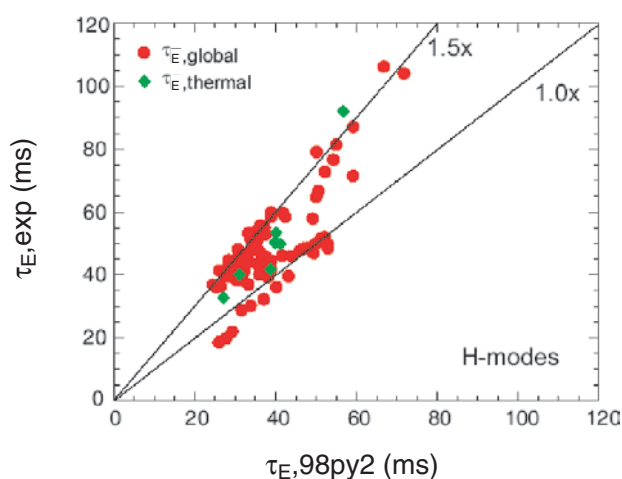


Figure 3. Global confinement trends in NSTX. The red points are H-mode points where the confinement time was computed using the EFIT global stored energy and the NBI injected power. The green points are some initial corrections with TRANSP to include only the thermal components and NBI deposited power removing the prompt loss.

significant non-inductive current fraction of $\sim 60\%$ in NSTX as shown in figure 4. These discharges had good overall plasma performance parameters of $\langle\beta_T\rangle \approx 16\%$, $\beta_N \approx 6$, $HH \approx 1.3$, $H_{89P} \approx 2.5$ or $\beta_N \times H_{89P} \approx 15$. Moreover, due to the low loop voltage (~ 0.1 V compared to 0.5 V for typical NBI heated discharges), the high poloidal beta regime was maintained for times larger than τ_{skin} or about $5\tau_E$ [9]. It is encouraging to note that these dimensionless plasma parameters achieved in NSTX (except for the pulse length) are already approaching those needed for a CTF. Since the 2000 IAEA meeting, the H-mode database for STs has been expanding rapidly. The H-mode operation is now routine on NSTX and MAST. The observed H-mode power threshold has been coming down and it is now well below 1 MW, giving reasonable confidence that the H-mode can be accessed in future devices such as NSST [13, 14]. It should also be noted that the H-mode access has facilitated the attainment of high beta regimes in NSTX by providing broader pressure and current profiles [11], which are favourable for MHD stability. These high performance ST plasma parameters, already obtained at $I_p \sim 1$ MA, suggest promising operating regimes for NSST and, if they can be extended to the 5–10 MA range on NSST, bode well for the development of ST fusion energy based on a compact ST CTF facility and an eventual ST Demo.

2.4. Base physics design parameters of NSST

To guide in the selection of a design point, which can meet the requirements of the NSST mission, a systems code was developed and a parametric study was performed [15]. Many promising design points have emerged. The tokamak simulation code (TSC) was also used to validate the systems code findings. In figure 5, the targeted NSST parameter space is shown. The current sustainment regime at $B_T = 1.7$ T ($\tau_{\text{pulse}} = 20$ s $\sim 3\tau_{\text{skin}}$) is ideal for investigating the

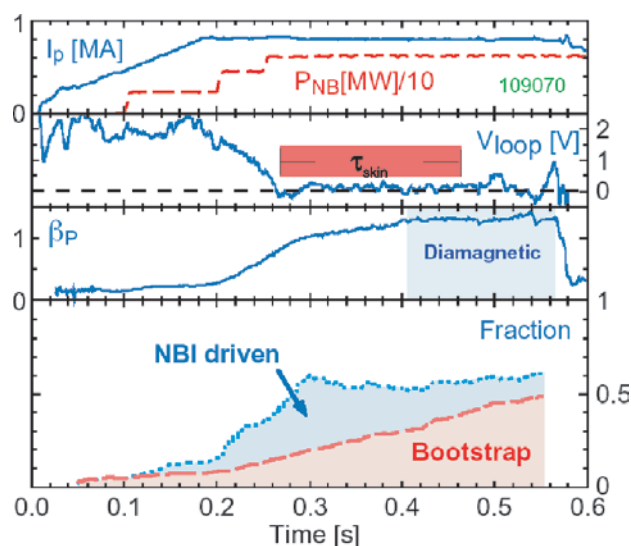


Figure 4. The discharge evolution of the high β_p shot in NSTX. The high beta poloidal discharge is obtained with significant $\sim 60\%$ non-inductive current drive with the loop voltage remaining very low at ~ 0.1 V. The bootstrap current fraction gradually increases in time due to a similar density rise. The high beta poloidal regime is maintained for times larger than the resistive skin time. The discharge becomes diamagnetic after 400 ms.

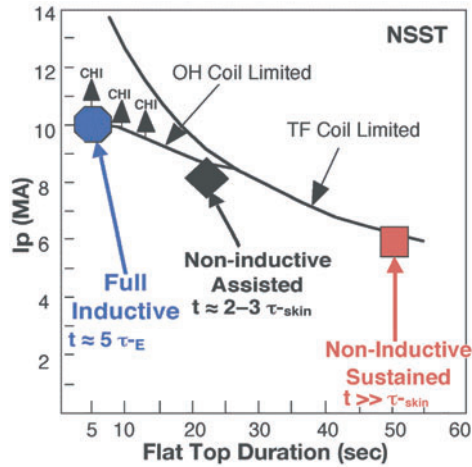


Figure 5. NSST operating design points: three main operating regimes are shown. The 50 s non-inductively sustained regime is aiming to develop Ohmic solenoid free start-up and current sustainment concepts at multi-MA range for a pulse length much greater than the plasma skin time, which is directly relevant for the design of CTF. The non-inductively assisted regime operates at a higher plasma performance of $Q \sim 0.5$ for 20 s or 2–3 skin times. This operation may use half-swing induction to ramp-up the current followed by a strong non-inductive current drive for sustainment. The full inductive region employs double-swing induction to reach a high current and high performance region of $Q \sim 2$ for 5 s or about 10 energy confinement times. This regime is a candidate for tritium operation to study α -particle physics at high beta, relevant for Demo.

Table 2. Key plasma and device parameters for full inductive and non-inductive sustained regimes.

	Full Inductive	Non-inductive sustained
B_T (T)	2.6	1.15
β_T (%)	13.3	26.3
β_N (%)	3.2	4.64
$\langle n_e \rangle$ (10^{20} m^{-3})	2.1	1.0
f_{GW} (%)	63.3	50.7
$\langle T_e \rangle$ (keV)	5.5	4.5
τ_{skin} (s)	9.3	4.9
$HH(98\text{phy}2)$	1.4	1.4
τ_E (s)	0.7	0.36
Q	2	0.25

CTF-like regimes at moderate Q . Here, a half-swing of the Ohmic heating (OH) coil (from initial pre-charge current ramped down to zero) can start-up the plasma. Another important research aim of NSST is to demonstrate multi-MA solenoid-free start-up. A demonstration of multi-MA start-up is essential to establish a design base for a toroidal CTF without an OH solenoid. To allow a sufficient pulse time to investigate such non-inductive scenarios, NSST can operate for 50 s at 6 MA with $B_T = 1.1$ T. Finally, to explore a wider ST plasma parameter space, the NSST device can operate in a purely inductive mode up to 10 MA, with $B_T = 2.7$ T, with a 5 s flat-top using the full OH swing, where $Q = 2$ performance can be expected with $HH = 1.4$. This operating mode will enable an exploration of α -particle related physics in high β plasmas for $\tau_{pulse} \sim 5\tau_E$. A TSC simulation for the 10 MA inductive case has yielded $Q \sim 2$ with somewhat relaxed $HH = 1.3$ due to the plasma profile effect. In table 2, the key parameters are listed

for the full inductive and non-inductive sustained cases shown in figure 4. As shown in the table, the NSST base parameters require relatively modest plasma beta and Greenwald density parameters.

3. NSST device design

3.1. NSST device design overview

To achieve the NSST mission, a flexible NSST device design was developed [16]. An isometric view of the NSST device and a device cross sectional view are shown in figures 6 and 7. The magnets are liquid nitrogen cooled to allow long pulse as well as high performance operation. To facilitate quick progress for the NSST research programme, an innovative Ohmic solenoid is designed into the baseline centre-stack design to deliver sufficient flux (~ 15 Wb) for 10 MA operations with full swing and 6 MA operations with half swing (~ 8.5 Wb). As shown in figure 7, with the in-board PF-1 coils, a strong plasma shaping capability (elongation $\kappa = 2.7$, triangularity $\delta = 0.6$) is incorporated in the design. In figure 8(a), a TSC simulation of an inductively driven 10 MA plasma cross-section is shown, confirming the strong plasma shaping capability with $\kappa = 2.7$ and $\delta = 0.6$. In figure 8(b), the no-wall MHD stability limit is shown as a function of δ or several values of κ for the plasmas with $\sim 50\%$ bootstrap current fraction. As shown in the figure, the beta limit of $\beta_T \sim 30\%$ can be reached without the benefit of the stabilizing plates for $\kappa = 2.7$ and $\delta = 0.6$. It should be noted that the expected range of the NSST base β_T values are indicated in the figure, which are well below the $\beta_T \sim 30\%$ limit. For example, the $Q = 2$ high performance regime can be achieved with a plasma beta of only about 13% (see table 2). This shows that Q can be raised further (if, for example, the confinement improves to above $HH = 1.3$ – 1.4) without exceeding the beta limit. An increased plasma beta is also desirable for increasing the bootstrap current fraction, which is an important element of the plasma sustainment in advanced ST scenarios. If the wall stabilization can be utilized, the β_T value can be increased further towards 45%, which is important for advanced ST operations with high bootstrap fractions, relevant for Demo and power plants. To explore the advanced ST regimes, NSST is designed with tightly fitted stabilizing plates to access simultaneously the high β_T and β_N (high bootstrap current fraction) regimes, as shown in figure 7. The outboard PF coils are placed sufficiently far from the plasma to reduce local shape distortions. The device is designed with a removable centre-stack to facilitate remote maintenance and allow for the possibility of future upgrades. The present NSST design utilizes a TFTR-like site with a peak electrical power of 800 MW and energy per pulse of 4.5 GJ and long pulse auxiliary heating and current drive systems (30 MW of NBI and 10 MW of RF). To explore the alpha-physics in high beta plasmas, the existing tritium handling capability can be utilized.

3.2. TF coils

The NSST TF coil consists of 96 standard turns with removable joints. A schematic of the TF coil is shown in figure 9. The TF joint details are shown in figure 10. Like NSTX, NSST features a demountable TF coil design, which permits the ‘centre-stack’

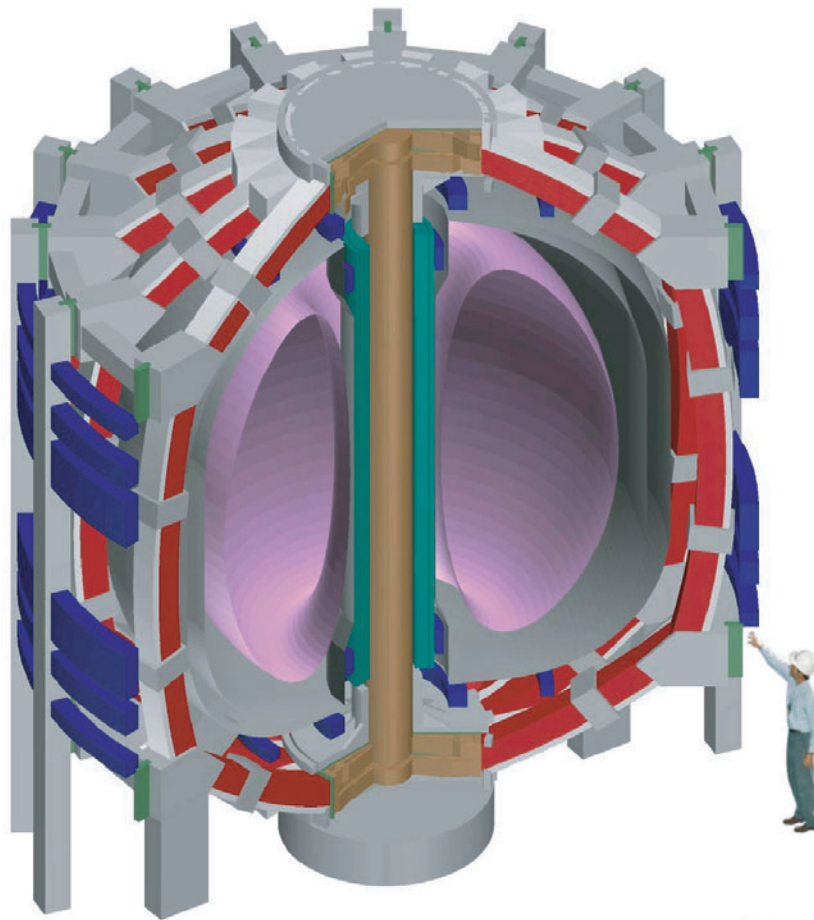


Figure 6. Isometric view of NSST. The outer TF is depicted in red and the poloidal coils are depicted in blue. The brown central column denotes the inner TF legs. The green cylinder around the inner TF depicts the Ohmic solenoid. The stainless steel vacuum vessel is double walled and filled with neutron absorbing material. The double-walled vacuum vessel and the supporting structures are shown in grey.

(i.e. the part which contains the TF inner legs, OH coil sections, and PF1a coils; the casing also serves as the inner wall of the vacuum vessel and PFCs) to be removed and installed as an integrated unit, as shown in figure 11(a). The TF inner legs, consisting of 96 standard OFHC copper (Cu) turns, of wedge shaped conductors, arranged in two layers, are cooled by liquid nitrogen (LN_2) via paths extruded in the conductors. Each of the 96 TF conductors has an independent cooling path. The liquid nitrogen enters from one end of the inner TF conductor and enters a corresponding outer TF conductor at the other end through a connecting hose and then returns to the original location through an outer TF conductor. Turn-to-turn transitions in the two joint layers proceed in opposite directions so as to cancel the net toroidal current. The assembly is fabricated in a fashion similar to NSTX, except for the fact that a high temperature, high shear stress cyanate ester resin insulator is used since the inner TF coil is designed near the stress limit against the torsional shear stress due to the Ohmic solenoid. Torsional loads arising from the OH radial field crossing the TF current are reacted through the outer TF coil legs. The TF joint design requires some innovation to satisfy the stringent mechanical and electrical requirements while facilitating simplified joint dismantling and reassembly for the TF centre-stack removal and installation. One possible type of joint design is shown in figure 10. The radial flags are

wedged into a hub assembly to form a monolithic structure. The connectors are slightly flexible in the radial direction to avoid the development of a large radial force on the flags, and to allow the outer legs to rest against their support structure. Torsional loads arising from the OH radial field crossing the TF current are reacted through the outer TF coil legs. Radial flags and connectors are used to make the joints between the inner legs and the outer legs (as shown in figure 10).

The current density in the outer legs is relatively low and the temperature rise is less than 10°C per pulse. They are cooled by the exit flow of nitrogen (gas initially; liquid at full cool-down) routed through extruded paths in the outer leg conductor. As shown in figures 7 and 9 the shape of the outer legs is chosen such that the outward magnetic pressure due to the TF current crossing with the TF field results in a constant tension in the support strap, with minimal vertical tension imposed on the inner legs. Compression rings are used to adjust the constant tension shape to suit the desired height of the TF coil assembly. With the constant tension and moment-free shape, the outer legs and associated support structure can be made relatively flexible in the axial direction, thereby allowing the thermal expansion and contraction of the inner leg assembly without generating large stresses. The out-of-plane forces on the outer leg due to the effect of the radial component of the TF current and the vertical field of the PF coils are transmitted

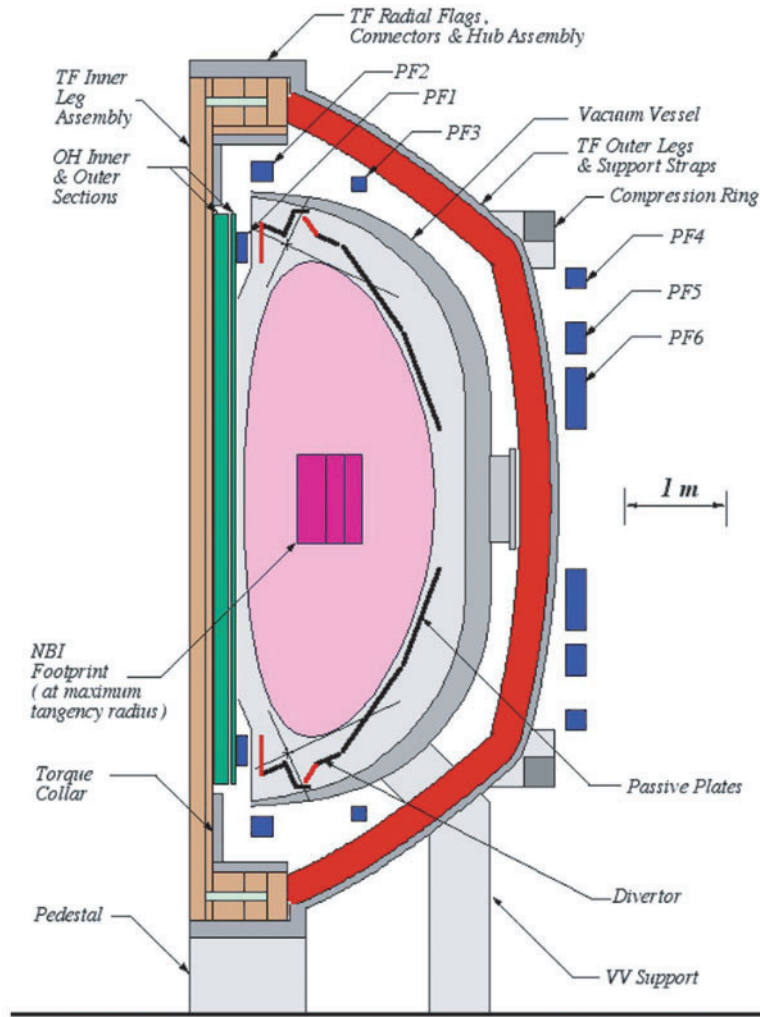


Figure 7. NSST device cross section: the vacuum vessel contains neutron absorbing material as a partial shield to minimize the external activation. The passive plates are for the resistive wall stabilization with rotation.

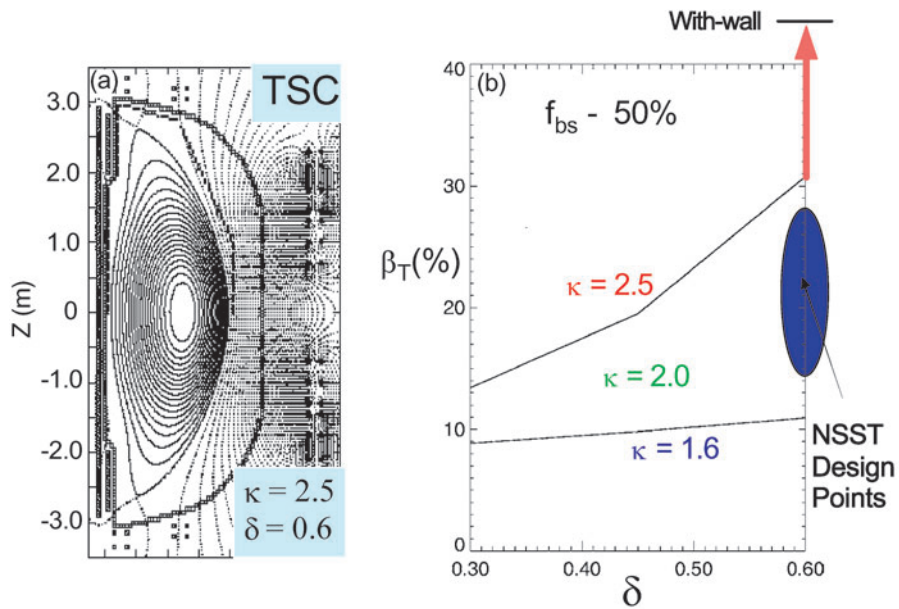


Figure 8. NSST plasma MHD stability limit: (a) TSC simulation of 10 MA inductively driven highly shaped plasma. (b) No-wall MHD stability dependence of triangularity for various elongations with the bootstrap current fraction of ~50%.

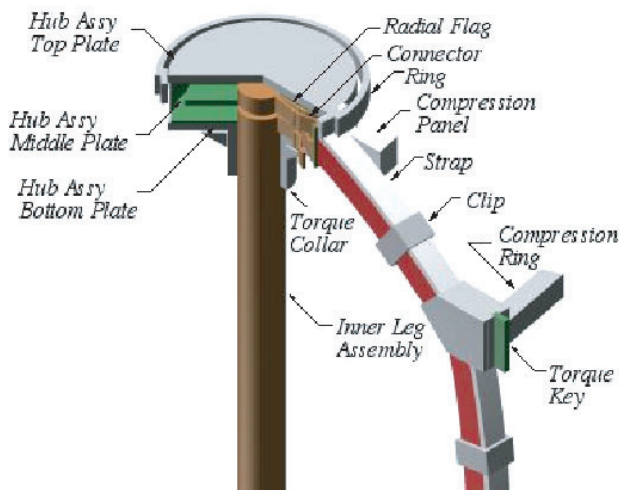


Figure 9. NSST toroidal coil schematics. The TF consists of 96 standard turns with removable joints. The inner TF conductor is wrapped with cyanate ester insulation which has higher shear strength at elevated temperatures and better radiation resistance compared to standard epoxies. The torsional loads from OH are reacted through torque collar and TF joint flags to the hub assembly and to the outer TF support. Constant tension outer legs with compression rings and flexible straps are envisioned.

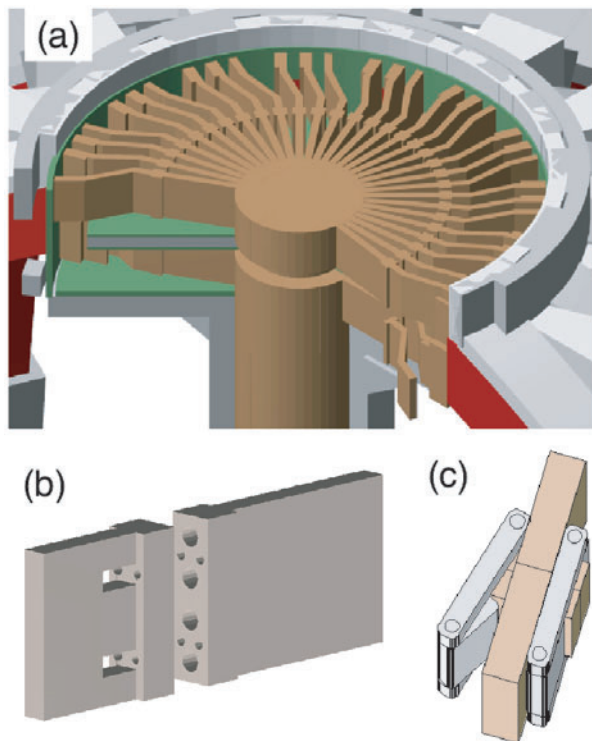


Figure 10. TF joint details: (a) TF joint overview schematic. Two layer 96 joint design. (b) Flag-to-connector joint concept using recessed flag studs and cut-outs for fasteners. (c) Alternate NSST flag-to-connector joint concept using over-centre clamps to facilitate remote handling.

to the strap assembly via the compression panels and straps. The intrinsic torsional rigidity of the strap/compression ring structure is supplemented by mechanical keys which transmit torsional loads to the ‘cage’ surrounding the machine, which

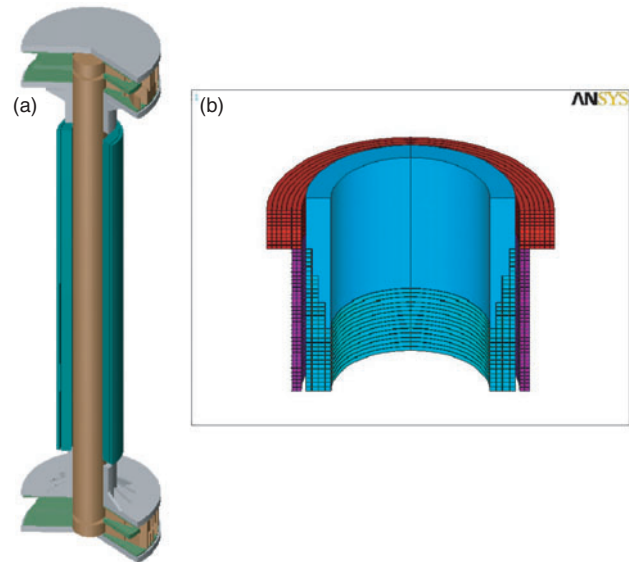


Figure 11. OH solenoid design. (a) Two-layered OH solenoid design is shown in green around the inner TF bundle (in brown). The outer OH layer is made of oxygen-free copper and the inner OH layer is made out of beryllium copper. The OH coil sections are cooled by LN₂ flowing through the annular regions between the OH and TF coils and between the OH sections. (b) A properly contoured OH solenoid end design to control the flaring of the OH fringing field pattern can reduce the local $j \times B$ force stress on the inner TF bundle.

is formed by PF coil support columns and compression rings, as shown in figure 7. Shear panels between the PF support columns will be added if further analyses indicates the need for additional torsional stiffness.

3.3. OH solenoid and poloidal field coils

In figure 11(a), the Ohmic solenoid as a part of the centre-stack assembly is shown. A two-part OH coil design is used, consisting of two concentric sections, with different current densities in each section to increase the total available flux. The sections are connected in series and carry the same current per turn. The outer section is much less stressed compared to the inner one. Since the outer coil has a much longer path, it uses a standard oxygen-free copper (Cu) conductor, which is operated to its thermal limit. The inner radius of the outer section, which is the highest field point, is chosen such that the hoop stress is at the allowable limit for copper. The outer OH coil section is, therefore, both thermal and stress limited, simultaneously. The inner section, operating at a much higher field level compared to the outer one, requires special strength copper. Because of its exceptionally high strength and relatively high conductivity a beryllium copper (BeCu) alloy is used, and the inner layer reaches its thermal limit before it reaches its allowable stress. While one could further optimize the strength and conductivity of the alloy used for the inner OH coil to make it simultaneously stress and thermal limited, the decision to use BeCu is largely based on its extensive availability and well-known material properties. The OH coil sections are cooled by LN₂ flowing through the annular regions between the OH and TF coils and between the OH sections. The long path length of the OH coil winding

makes it impractical to cool the coil using liquid nitrogen cooling through the conductor, as in the case of TF. The bipolar swing of the OH current is asymmetric about zero to exploit the higher strength of the conductors at cold temperatures during the first swing; the ratio of the first swing of current to the second swing equals 1.8. The end of the OH solenoid can be contoured as shown in figure 11(b) to tailor the flaring out of the OH fringing field to reduce the local $j \times B$ torsional force on the inner TF bundle by a factor of two. This feature does add to the complexity of the OH solenoid; however, it remains an option, which can be used if necessary in the final design.

The PF coil system consists of six coil pairs symmetric about the device midplane. The current per turn is 24 kA in all circuits, based on the rating of TFTR-like power supplies. The PF coil design is relatively conventional due to its simple geometry and modest performance requirements.

3.4. Vacuum vessel and PFCs

A double walled vacuum vessel with integral shielding is used on NSST. The vessel is fabricated of 316SS. The inner wall is 19 mm thick and the (less stressed) outer wall is 16 mm thick. Welded ribs are provided between the inner and outer walls to stiffen the structure. The space between the walls is filled with 60% 316SS balls and 40% water to provide adequate shielding of device externals to the expected neutrons during the D–T operation. Ports are based on 16-fold symmetry. Four (4) midplane ports are assigned to the tangential access for the NBI injectors as shown in figure 12. Eight pairs of 6" diameter ports are included to accept feed-throughs for an eight strap RF antenna subtending $8 \times 7.5^\circ = 60^\circ$. The remaining nine rectangular midplane ports are 61 cm wide and 91 cm high. Sixteen 30.5 cm diameter ports are provided on the upper and lower domes; that is, a total of 32. Ample plasma access is provided for plasma profile diagnostics to facilitate NSST

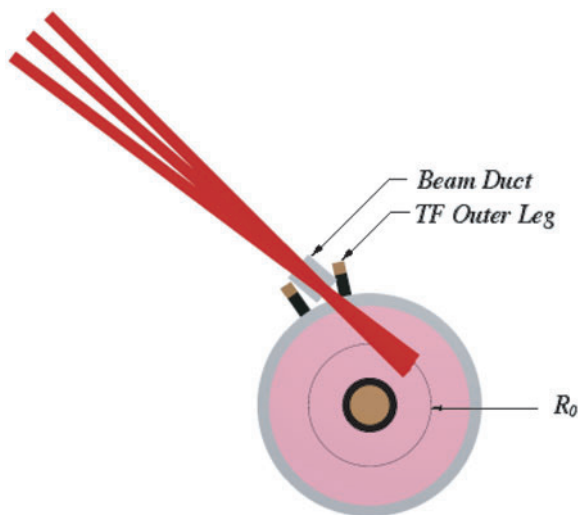


Figure 12. Tangential NBI access view: relatively slender TF outer legs enable the tangential NBI access. One of four NBI beam boxes is envisioned to be placed in the counter-direction to provide momentum input flexibility. The beam angles will be chosen to optimize the physics flexibility.

research. The inner wall of the vacuum vessel (i.e. the centre-stack casing) is formed by the 5 mm thick Inconel ‘centre-stack casing’. Bellows assemblies and flanges are provided to allow for differential thermal expansion with respect to the outer vacuum vessel. The power and particle handling is a challenging issue for NSST and it is anticipated that the PFCs will be actively cooled for heat removal. The same cooling path will be used to heat the tiles for high temperature bakeout. The initial PFC material used will be graphite tiles, due to the extensive operational experience with them. However, more advanced PFCs can be considered for those D–T operations in which tritium retention may become an issue.

3.5. Remote maintenance

The NSST’s unique configuration permits a relatively simple remote maintenance system. The doubled walled vacuum vessel is an effective shield such that work restrictions around the machine should be similar to those of the large D–T tokamak experiments, such as TFTR. So, we can utilize the extensive D–T experience from those tokamak experiments including many of the procedures. Remote maintenance is, however, required for the internal components after the initiation of the D–T campaign for NSST. The ST geometry provides a unique opportunity for relatively simple remote maintenance. It is envisioned that the remote maintenance will be performed with the centre-stack removed from the device, as illustrated in figure 13. The centre-stack is lowered into the basement, as shown in figure 13(a). After the removal of the centre-stack, the access to the vacuum vessel internals becomes rather straightforward since an opening of about 2 m in diameter becomes available. Through this opening a simple robotic arm with less than 3 m reach on a movable (vertically and rotatable) platform placed at the machine centre can reach the entire internal surface of NSST as shown in figure 13(b). The remote maintenance of the removed centre-stack can be also performed with a relatively simple set-up as shown in figure 13(c). With the centre-stack placed on a rotatable pedestal, a relatively short maintenance robotic arm system placed on a vertically moveable platform allows remote maintenance of the entire centre-stack surface. The removable centre-stack thus allows a cost effective maintenance and repair of the internal vacuum vessel component as well as the centre-stack. Since the cost of such remote maintenance systems (the platforms and remote arms) is relatively modest, they might be useful not only for the D–T campaign but also during the initial D–D phase of operations. An early introduction of such remote maintenance systems would increase the installation precision and reduce the safety risks to personnel working inside the relatively large vacuum vessel as well as on the relatively tall centre-stack.

4. Physics tools and research opportunities

4.1. Heating and current drive

The baseline heating and current drive system for NSST is the 110 keV–30 MW NBI system and a 10 MW of ion cyclotron range of frequency (ICRF) and high harmonic fast wave (HHFW) system. The choice of NBI and ICRF is based on the relatively extensive experience and theoretical understanding

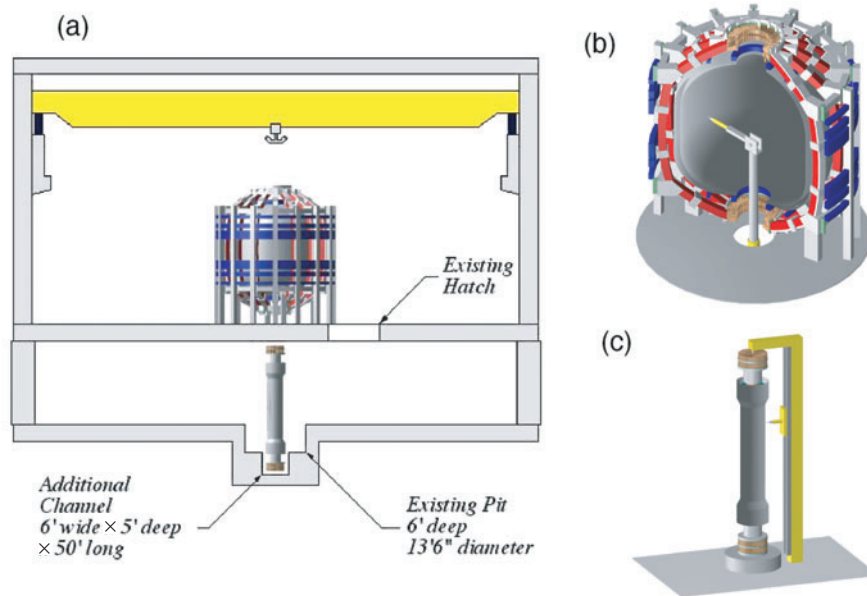


Figure 13. NSST remote handling schematics: (a) NSST centre-stack being lowered into the basement for maintenance. (b) A set-up for internal vacuum vessel component maintenance. (c) A set-up for centre-stack maintenance.

of both heating and CD systems in Tesla-range experiments. The existing 30 MW NBI and 10 MW ICRF facilities are well developed and can be implemented at low cost and with low risk. The NBI beam ion confinement is expected to be excellent in NSST even accounting for possible losses due to MHD activities, such as TAEs and fishbones. The 30 MW NBI is expected to provide reliable baseline heating and current drive. The NBI also provides other important functions such as imparting toroidal momentum to drive toroidal rotation and substantial core fuelling with a rate of $\sim 2 \times 10^{21}$ particles s^{-1} . It should be noted that NBI could also provide a platform for advanced plasma diagnostics.

The physics issues related to the ICRF/HHFW system are more challenging due to the three different operating magnetic field regimes. For the high performance D–T burning regime operating at $B_T = 2.6$ T, the main objective of ICRF is to heat the plasma core as needed. For this case, the well developed He₃–D or $2\Omega_T$ scenario appears to be most suitable with frequency in the range $f \approx 20$ –25 MHz. For lower field, long pulse, non-inductive operations, ICRF will be used as a plasma start-up and current drive tool. Since this regime is expected to operate mainly with deuterium, second or third harmonic deuterium heating can be expected. In this regime while the electron Landau and magnetic pumping absorption processes can be strong due to the relatively high beta value of the plasmas, one must also estimate the power absorbed by deuterium cyclotron harmonic damping. One could also consider going towards a higher frequency of the HHFW to avoid ion absorption.

4.2. The NBI induced plasma rotation

One of the long term goals of NSST research is to access the advanced ST regimes. If successfully demonstrated, it could favourably impact the operational scenarios of the CTF by supporting higher performance operations. In addition, it

would support the design of Demo and power plants operating at higher beta. To foster advanced ST research, we have chosen tangential NBI as a reliable means to impart toroidal momentum to the plasma together with tightly fitted stabilizing plates. In figure 12, the NBI top view geometry is shown. In figure 14(a), the injected radial toroidal torque profile as calculated by TRANSP is shown where four co-injected beam lines are used. The resulting toroidal rotation velocity is shown as a function of the major radius (figure 14(b)). Here the toroidal angular momentum diffusivity is assumed to equal the neoclassical ion thermal diffusivity. In NSTX, the toroidal angular momentum diffusivity of about $\frac{1}{3}$ of the neoclassical values has been observed [12]. Therefore, the neoclassical-like angular diffusivity assumption used for NSST is relatively conservative. As shown in the figure, the toroidal rotational speed could reach 600 km s^{-1} or 35% of the local Alfvén velocity in NSST. Since the rotational speed required for the RWM stabilization is typically a few per cent of the Alfvén velocity, the generation of sufficient toroidal rotation should be readily achievable in NSST. We can, therefore, consider placing one of the four NB injectors in the counter-direction to introduce additional physics flexibility. The remaining three NB injectors will be installed in the co-direction at various injection angles and tangency radii. This will potentially allow finer control of the rotational velocity per given injected NBI power as well as control of the heating and current drive profiles and velocity sheared layer locations for the ITB formation to control, for example, the pressure profile.

4.3. Solenoid-free start-up

The demonstration of a multi-MW level solenoid-free start-up current is a central topic for NSST. At present, NSTX is investigating coaxial helicity injection (CHI) plasma current start-up, which has succeeded in driving about 400 kA of

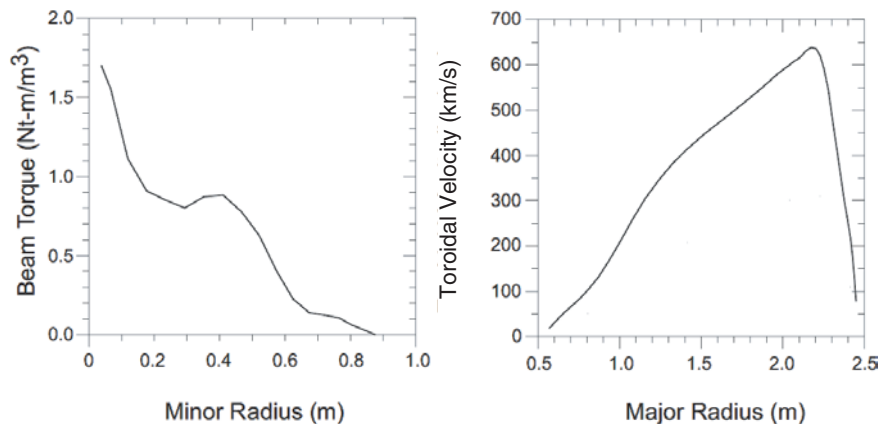


Figure 14. TRANSP simulation of NBI induced toroidal rotation: (a) Toroidal torque provided by NBI beam. (b) Resulting plasma toroidal rotation profile.

toroidal current with injection of 27 kA at about 700 V bias voltage [6, 17]. Recently, on the HIT-II device, an experiment was conducted to show significant Ohmic volt-second savings with the initial application of CHI [17]. While CHI is still under development, the trend from HIT-II to NSTX seems to show a favourable scaling of a factor of two in the current multiplication (i.e. the ratio of the generated toroidal current to the injected CHI current). The expected CHI requirement increases with the desired plasma start-up current and the plasma size but decreases with the plasma temperature due to slower current (or helicity) dissipation. Using similar scaling from HIT-II to NSTX, the current multiplication can be expected to be about three times larger on NSST compared to NSTX for the same injector flux and voltage. In addition, by going to higher voltages (2–3 kV), which is likely to be required for operation at much higher TFs in NSST compared to NSTX, it appears to be feasible to drive 5 MA of toroidal current with an injection current of only about 30 kA. It is, therefore, important to understand this scaling through experiments as well as through three-dimensional numerical simulations before finalizing the CHI design for NSST. The fact that the NSST centre-stack is dismantlable should permit the incorporation of the required CHI insulator if the CHI technique can be shown to be extendable to multi-MA level plasma currents.

With its long pulse length of 50 s, NSST can also test other innovative, non-inductive current drive techniques, such as bootstrap over-drive using rf based heating as invoked in the ARIES-ST/AT study. The recent JT-60U experiment on non-Ohmic plasma start-up used modest Ohmic induction, rf and NBI current ramp-up, NBI heating induced bootstrap over-drive, and vertical field ramp-up to obtain $I_p = 600\text{--}700$ kA, a very encouraging result [18]. The NSST could further develop this technique towards multi-MA regimes, which are necessary for the design and construction of a CTF facility. On NSST, we can utilize a modest amount of ECH or electron Bernstein waves (EBW) power [19] to initiate the plasma discharges and the 10 MW ICRF system in a HHFW heating and current drive mode [20] to ramp-up the plasma current. After the plasma current reaches an adequate level for the NBI confinement (>1 MA), the 30 MW NBI heating can be turned on to heat and densify the plasma to a high-poloidal-beta/high bootstrap current fraction to reach a multi-MA

Table 3. Key physics dimensionless parameters for representative ST devices.

	NSTX	NSST	CTF	ARIES-ST
v^*	0.2	0.04	0.02	0.015
a/ρ_i	35	130	108	140
$\langle\beta_T\rangle$	0.35	0.4	0.2–0.4	0.5
$V_{\text{NBI}}/V_{\text{Aif}}$	3	0.7	—	—
V_α/V_{Aif}	—	4.4	5.8	5

current. The optimization of the poloidal/vertical fields as done for the JT-60U is also a very important part of this study. The demonstration of the solenoid-free start-up technique is considered to be essential for an ST-based compact CTF as well as for power plants.

4.4. α -particle physics

In table 3, some relevant dimensionless physical parameters are listed for representative ST devices. In terms of the α -particle related physics, a key dimensionless parameter is V_α/V_{Aif} , which is about 4–5 for NSST, but also has similar values for future devices such as ST-based CTF and the ARIES-ST power plant. This value is also comparable to the values reached on NSTX with NBI, where $V_{\text{NBI}}/V_{\text{Aif}} \approx 3$. On NSTX, NBI heated discharges indeed yielded a variety of high frequency MHD modes including toroidal Alfvén eigenmodes (TAEs) in the 100 kHz range and compressional Alfvén eigenmodes (CAEs) in the range of a few MHz range (starting from close to half of the deuterium cyclotron frequency). In NSTX, CAEs are not observed to cause any NBI ion particle losses but there is an interesting theoretical prediction of CAEs stochastically heating bulk ions [21]. This prediction was stimulated by the apparent observation of unusually high ion temperature discharges on NSTX during NBI [12]. If proved to be true, this direct ion heating by α -particles can further enhance the high Q operational regimes in ST reactors. The NSST device and its physics diagnostic capabilities should, therefore, yield important reactor relevant α -particle related physics data as well as the isotope scaling in high beta toroidal plasmas for the first time. In the 10 MA NSST discharges, the α -particle orbits are estimated to be relatively well confined [22].

5. Summary and future plans

The ST concept can contribute effectively to the development of fusion energy (i.e. NSTX/MAST, NSST, CTF, and Demo). The ST development path is complementary to the tokamak-based burning plasma experiments as it focuses on a compact CTF facility and exploration of higher toroidal beta regimes for Demo and power plant reactors. The CTF facility can provide a test bed for the development of blanket modules and other fusion core components, exposing them to high neutron wall loading and accumulated fluence. As an ST PE level experiment, the NSST facility can provide the necessary physical basis for the design and construction of a compact ST-based CTF, while developing more advanced physics scenarios for CTF, Demo and ST power plants. To support its mission, the NSST facility, with up to 10 MA of plasma current, is designed with advanced physical features, such as strong plasma shaping and wall mode stabilizing plates, as well as physics tools including the NBI system to drive sufficient toroidal rotation and rotational shear flows for improved stability and confinement, and with excellent diagnostic access to facilitate physics research. Tritium operation will enable α -particle and isotope scaling research at high beta for the first time providing a valuable database for an attractive Demo design. The dismantlable centre-stack design can facilitate remote maintenance of the NSST internal hardware.

Acknowledgments

This work was supported by US Department of Energy under contracts DE-AC05-00OR22725 and DE-AC02-76CH03073, and grants. Thanks are due to the NSTX Research Team for providing pertinent data for the NSST design, R. Goldston and R. Hawryluk for advice and encouragement, and S. Jardin for expert help in the analysis codes.

References

- [1] Peng M. and Hicks J.B. 1991 *Fusion Technology 1990* vol 2 (Amsterdam: Elsevier) p 1287
- [2] Peng M. *et al* 1998 *17th IEEE/NPSS Symp. on Fusion Engineering 1997* vol 2, p 733
- [3] Sviatoslavsky I.V. *et al* 1999 *Fusion Eng. Des.* **45** 281
- [4] Abdou M.A. *et al* 1996 *Fusion Technol.* **29** 1
- [5] FESAC Panel of Development Path. A Plan for Development of Fusion Energy *Preliminary Report* to FESAC, issued in March 2003
- [6] Goldston R.J. 1984 *Plasma Phys. Control. Fusion* **25** 874
- [7] Synakowski E. *et al* 2003 *Nucl. Fusion* **43** 1653
- [8] Lloyd B. *et al* 2003 *Nucl. Fusion* **43** 1665
- [9] Menard J. *et al* 2003 *Nucl. Fusion* **43** 330
- [10] Gryaznevich M. *et al* 1998 *Phys. Rev. Lett.* **80** 3972
- [11] Sabbagh S. *et al* 2002 *Proc. 19th Int. Conf. on Fusion Energy 2002 (Lyon, 2002)* (Vienna: IAEA) (CD-ROM) file EX/S2-2 and <http://www.iaea.org/programmes/ripc/physics/fec2002/html/fec2002.htm>
- [12] LeBlanc B. *et al* 2002 *Proc. 19th Int. Conf. on Fusion Energy 2002 (Lyon, 2002)* (Vienna: IAEA) (CD-ROM) file EX/C5-2 and <http://www.iaea.org/programmes/ripc/physics/fec2002/html/fec2002.htm>
- [13] Maingi R. *et al* 2003 *Nucl. Fusion* **43** 969
- [14] Carolan P.G. *et al* 2002 *Proc. 19th Int. Conf. on Fusion Energy 2002 (Lyon, 2002)* (Vienna: IAEA) (CD-ROM) file EX/C2-6 and <http://www.iaea.org/programmes/ripc/physics/fec2002/html/fec2002.htm>
- [15] Jardin S.C., Kessel C.E., Meade D. and Neumeyer C.L. 2003 *Fusion Sci. Technol.* **43** 161
- [16] Neumeyer C. *et al* 2002 Spherical torus centre stack design *Proc. 19th IEEE/NPSS Symp. on Fusion Engineering (SOFE) (Atlantic City, NJ, January 2002)* IEEE No 0-7803-7073-2/02, pp 413–7
- [17] Jarboe T. *et al* 2002 *Proc. 19th Int. Conf. on Fusion Energy 2002 (Lyon, 2002)* (Vienna: IAEA) (CD-ROM) file IC/P-10 and <http://www.iaea.org/programmes/ripc/physics/fec2002/html/fec2002.htm>
- [18] Takase Y. *et al* 2002 *J. Plasma Fusion Res.* **78** 719–21
- [19] Efthimion P. *et al* 2002 *Proc. 19th Int. Conf. on Fusion Energy 2002 (Lyon, 2002)* (Vienna: IAEA) (CD-ROM) file EX/P2-12 and <http://www.iaea.org/programmes/ripc/physics/fec2002/html/fec2002.htm>
- [20] Ryan P. *et al* 2002 *Proc. 19th Int. Conf. on Fusion Energy 2002 (Lyon, 2002)* (Vienna: IAEA) (CD-ROM) file EX/P2-13 and <http://www.iaea.org/programmes/ripc/physics/fec2002/html/fec2002.htm>
- [21] Gorelenkov N. *et al* 2003 *Nucl. Fusion* **43** 228
- [22] Darrow D. *et al* 2002 *Proc. 19th Int. Conf. on Fusion Energy 2002 (Lyon, 2002)* (Vienna: IAEA) (CD-ROM) file EX/P2-01 and <http://www.iaea.org/programmes/ripc/physics/fec2002/html/fec2002.htm>